Electronic Supplementary Material (ESI) for Analyst.

Chip-based Potentiometric Sensor for Zika Virus Diagnostic Using 3D Surface Molecular Imprinting

Vincent Ricotta,[*a] Yingjie Yu,[a] Nicholas Clayton,[a] Ya-Chen Chuang,[a] Yantian Wang,[a] Steffen Mueller,[b] Kalle Levon,[c] Marcia Simon,[d] Miriam Rafailovich[*a]
[a] Department of Materials Science and Engineering, SUNY at Stony Brook, Stony Brook, NY 11794, USA
[b] Codagenix Inc., Farmingdale, NY, 11735, USA
[c] Department of Chemical and Biological Sciences, Polytechnic Institute of NYU, Brooklyn, NY 11201, USA
[d] Department of Oral Biology and Pathology, SUNY at Stony Brook, Stony Brook, NY 11794, USA
[*]E-mail: Vincent.Ricotta35@gmail.com, Miriam.Rafailovich@stonybrook.edu

Supplementary information

S1 Initial quality control testing of gold chips

The chip surface topography was characterized via atomic force microscopy (AFM). Fig. S1 displays 2D and 3D views on the AFM topographical scans of the bare gold chips. At the start of this work, all gold chips used were prepared by depositing chromium/gold films on silicon wafers (Fig. S1A and B).[1] These chips were produced by depositing an adhesion layer of chromium (~10 nm) on the silicon wafers prior to depositing a gold layer (~100 nm). Thin film deposition via electron-beam physical vapor deposition is an extremely sensitive technique. Changing a single parameter can drastically alter the physical and electrical attributes of the deposited films. Electron-beam physical vapor deposition is essentially about vaporization. One of the major issues revolving around the use of chromium in this deposition technique is that chromium sublimes instead of vaporizing once bombarded by the electron-beam. This makes surface topography reproducibility extremely difficult. The surface topography of the first batch of chromium/gold chips prepared was significantly different from that of the second batch prepared, with root mean square roughness (Rq) values of 0.57 ± 0.11 nm and 1.01 ± 0.03 nm, respectively. One of the other concerns with the methods initially used to prepare these chips was that deposition was performed under vacuum at 10^{-7} Torr. Although this is still considered high vacuum, it is best to deposit thin films under ultra-high vacuum to avoid any contamination of depositing evaporated particles along with molecules of remaining atmosphere gas in the evaporator chamber.

Titanium/gold chips were then prepared at the Advanced Science Research Center NanoFabrication Facility of the Graduate Center at the City University of New York. These chips were produced by depositing an adhesion layer of titanium (3.00 ± 0.05 nm) on the silicon wafers prior to depositing a gold layer (50.00 ± 0.20 nm). This yielded a more controllable deposition process and allowed for the reproducibility in chip surface topography. The gold nucleation of the titanium/gold chips fabricated appeared to be more homogenous than the chromium/gold chips prepared, with reproducible Rq values of 1.31 ± 0.55 nm (Fig. S1C). Thin film deposition for these chips were also performed under vacuum at $< 9 \times 10^{-8}$ Torr. This higher vacuum further prevents contamination of depositing molecules of remaining atmosphere gas in the evaporator chamber. For these reasons, the fabricated titanium/gold chips were used for the remainder of this work.

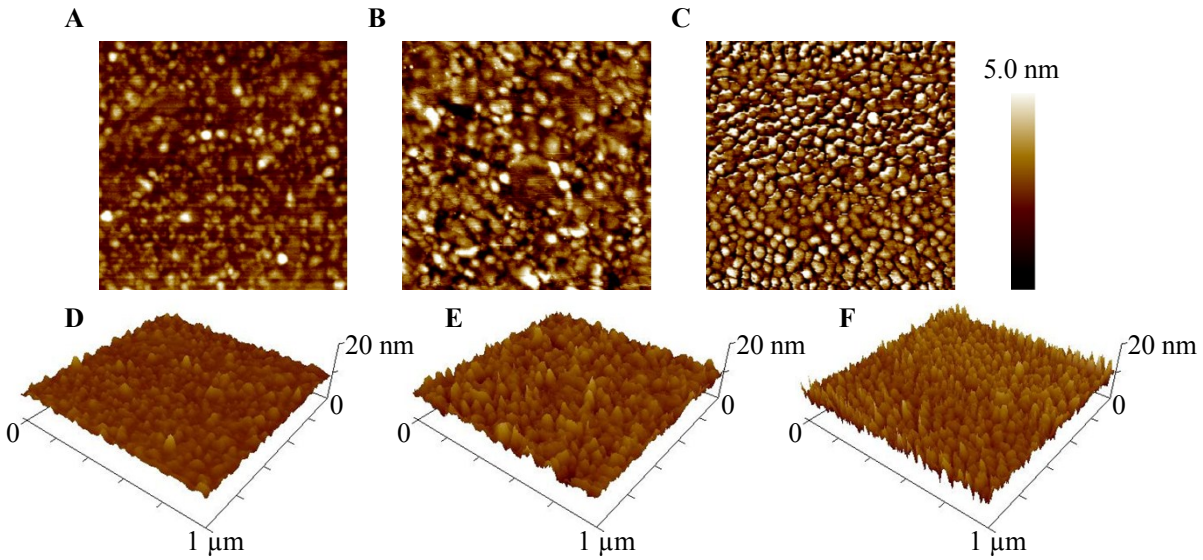

Fig. S1 AFM topographical scan of smooth gold surfaces via tapping mode. 2D AFM image of bare smooth chromium/gold (10 nm/100 nm) surfaces batch 1 (A), batch 2 (B), and titanium/gold (3 nm/50 nm) surface (C) with a 1 µm^2 scan size and Rq of 0.57 ± 0.11 nm, 1.01 ± 0.03 nm, and 1.31 ± 0.55 nm, respectively. 3D associated AFM image of A (D), B (E), and C (F).

S2 Optimization of thiol SAM formation

In order to optimize the MI technique for detecting ZIKV, the concentration of thiol needed for the MI process had to be determined first. It is well-known that the sulfur of alkanethiols form strong covalent bonds to gold as they produce SAM via the electron transfer reaction:[2-4]

$$M + H-S-R \rightarrow M-S-R + H^+ + e^- \qquad \textbf{Equation (1)}$$

During OCP analysis, the surface potential of the MI chip is measured against the surface potential of the reference electrode (Fig. S2). There was no additional current flown in this system through the external circuit, so any OCP response correlated to the chip surface charging during the SAM formation.[2] It was essential to determine the concentration of thiol needed to completely saturate and cover the working area of the chip in order for a successful MI chip. Using a concentration of thiol during the MI process that is less than the saturation concentration may lead to defects in the SAM or even open and exposed gold surface. These defects and exposed gold areas can result in undesired responses when measuring the change in OCP when re-adsorbing the target analyte to the MI chip. Defects and holes in the SAM may not be able to yield the lock-and-key complexes illustrated in Fig. 2. On the other hand, using a concentration of thiol greater than the saturation concentration may cause the thiols to precipitate in solution.

The average OCP response of titrating or adding thiol to the bare gold chips until fully saturated is plotted in Fig. S3. Here, DMSO was used as the buffer solution in the detection system instead of 1X dPBS in order to prevent any background OCP response from DMSO interacting with the gold chips. Serial dilutions of thiol/DMSO solutions were pipetted into the detection

system to measure the average OCP response of thiol adsorption on bare rough and smooth chips (3 each). The OCP response began to plateau between 25 – 100 μM of thiol for both the rough and smooth chips at 100 mV and 68 mV, respectively. However, alkanethiol SAM formation is dependent on time and concentration. As the concentration of thiol increases, the amount of adsorbed thiol to the gold chip surface increases. Increasing the time that the gold chip is exposed to the thiol solution will assist the thiol SAM to reorganize and eliminate any defects (Fig. S4).[4] Therefore, measuring the OCP response of titrating the bare gold chips with thiol solutions cannot solely determine the saturation concentration of thiol needed for the MI process.

The electrochemical analyses CV and EIS were performed to verify the saturation concentration of thiol on the gold chips. During CV, voltage is applied to the working electrode (gold chip) through the counter electrode (coiled Pt wire auxiliary electrode) and measured against the reference electrode (Ag/AgCl electrode), which remains constant. As the potential is cycled through the working electrode, a current is produced from the electron transfer between the gold chips and the redox active metal ions ($[Fe(CN)_6]^{4-}$ and $[Fe(CN)_6]^{3-}$). As the area of the working electrode decreases, the current produced from this redox reaction decreases[5].

Since alkanethiol SAM formation is dependent on time and concentration, imprinting time was kept constant at 2.5 hours [1, 3] as the thiol concentration was varied from 0.1 – 100 μM. Increasing the concentration of thiol in the imprinting solution caused more thiols to adsorb on the gold chips, where the SAM began to act as a barrier preventing the $Fe(CN)_6^{4-/3-}$ redox reaction from occurring.[1] As the concentration of thiol approached 10 μM and 100 μM, the redox peaks disappeared for both the rough and smooth gold chips (Fig. S5A and C). This disappearance correlates to the surface of the gold chips being saturated or completely covered by thiols. The thiols acted as a barrier and prevented the redox active metal ions from contacting the gold electrode surface, thus supporting the results of measuring the OCP response from titrating the gold chips with thiol/DMSO solutions.

During EIS, a fixed sinusoidal voltage is applied to the working electrode (gold chip) through the counter electrode (coiled Pt wire auxiliary electrode) in modulations of various frequencies, in which current then flows through the electrochemical cell and is recorded against the reference electrode (Ag/AgCl electrode). The current is recorded by the potentiostat and converted by the software via complex equations into impedance values for the real (Z') and imaginary (-Z") component throughout the selected frequency range.[6] In this EIS experiment (Fig. S5B and D), the bare rough and smooth gold chips produced linear lines in the Nyquist plot correlating with a mass diffusion-limited electron transfer process. As the thiols saturated the surface of the gold chips, these linear lines transformed to a well-defined semicircle correlating with a largely increased R_{ct}.[1] When preparing imprinting solutions with thiol concentrations greater than 100 μM, precipitates would form (not shown) thereby making the solutions incapable of being used to test the saturation concentration of thiol for the gold chips in the MI process. Based on these results, it was determined that a final thiol concentration of 100 μM would be implemented in the MI process.

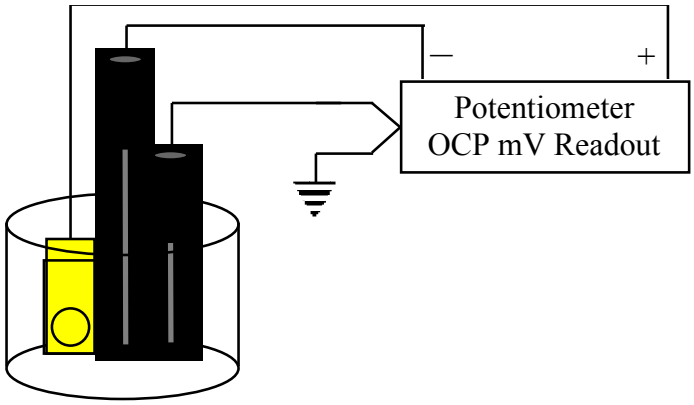

Fig. S2 Schematic illustration of the potentiometric biosensing system setup. A 3-electrode system was used; 1 Ag/AgCl electrode as the reference electrode, 1 Ag/AgCl electrode as the common ground electrode, and 1 MI chip as the working electrode. The 3 electrodes were all placed in a 10 mL beaker with 8 mL 1X dPBS continuously stirred with a magnetic stirrer and stir bar at 300 – 500 rpm. Known concentrations of analyte were added into the detection system, while the open circuit potential (OCP) was recorded in real-time using a potentiometer (Lawson Laboratories, Model EMF16).

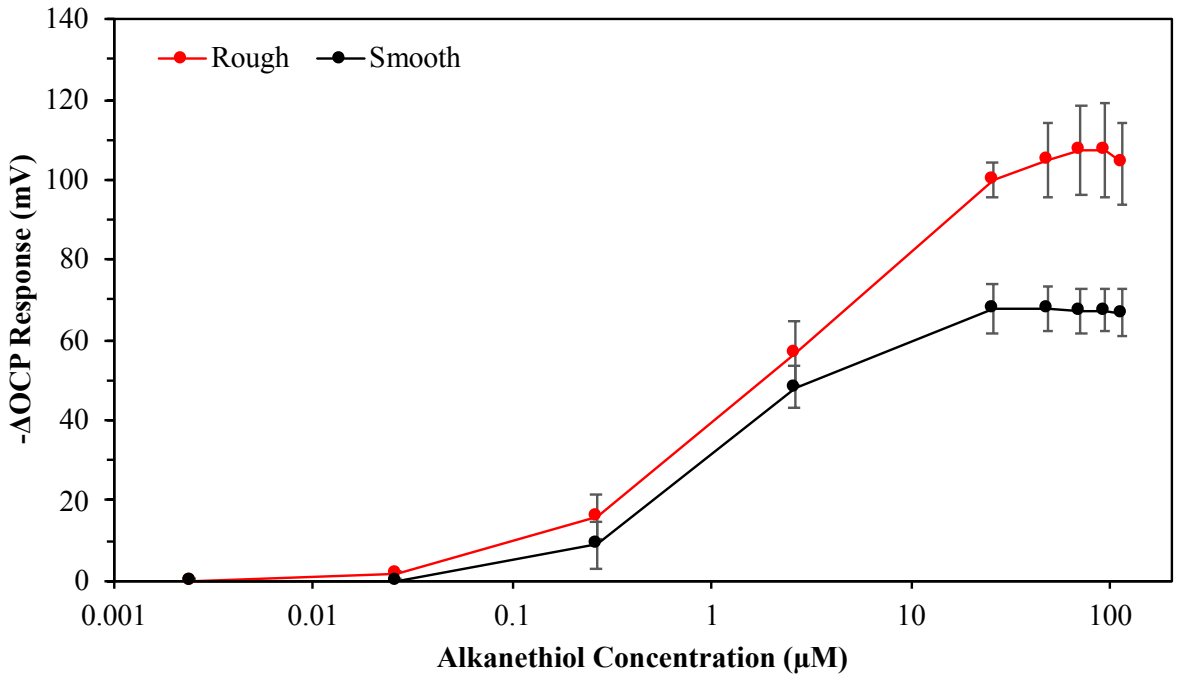

Fig. S3 Average potentiometric response of titration with thiol solution on bare gold chips. DMSO was used as the buffer, instead of 1X dPBS, for OCP measurements to prevent any background signal from DMSO on gold. Serial dilutions of thiol/DMSO solutions were pipetted into the detection system to determine concentration of thiol needed to fully saturate the surfaces of rough (red line) and smooth (smooth line) chips.

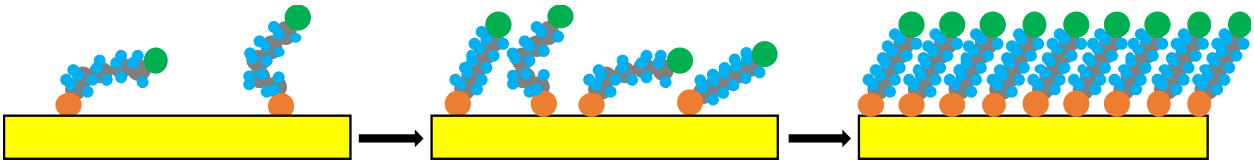

Fig. S4 Schematic illustration of alkanethiol self-assembled monolayer (SAM) formation on a gold surface. The alkanethiols adsorb to the gold surface forming a SAM that eventually covers the entire surface as time elapses or as the concentration of alkanethiols increases. Defects in the SAM will be reorganized and corrected as time and concentration increases as well.

S3 Optimization of washing method

The 3D surface MI model proposed that the substrate surface morphology forms a niche surrounding the target bio-macromolecule as the SAM adsorbs around the analyte in all directions. The sulfur of the thiol-terminal forms a strong covalent bond with the gold layer of the chips, thus making it extremely difficult to wash off the SAM with ease. The target bio-macromolecules interact with the thiol SAM through weak hydrogen bonding and Van der Waals interactions. Therefore, the imprinted analytes can be easily washed off without destroying the imprinted cavities, or lock-and-key complexes within the SAM. This washing process is crucial to a successful potentiometric readout when testing a sample for ZIKV re-adsorption.

Optimizing the washing method by completely washing off all imprinted analytes would produce the greatest OCP response. In order to test the washing method, rough and smooth gold chips were imprinted with ZIKV at 10^7 PFU/mL for 2.5 hours and then soaked in either 1 M NaCl, 1 M NaCl/0.1 % Tween 20, 3 M NaCl, or 3 M NaCl/0.1 % Tween 20 overnight to wash off the imprinted virions. The washed ZIKV MI chips were then reintroduced to ZIKV by pipetting serial dilutions of ZIKV from 1.2 x 10^5 to 5.5 x 10^6 PFU/mL into the detection system for a total of 3 times each for both the rough and smooth surfaces. The average -ΔOCP response for these MI chips are plotted in Fig. S6. When the ZIKV MI chips were reintroduced to ZIKV at 5.5 x 10^6 PFU/mL, the rough MI chips yielded average -ΔOCP responses of 1.49 ± 14.70 mV, 9.15 ± 14.24 mV, 55.20 ± 32.12 mV, and 32.15 ± 17.35 mV for the 1 M NaCl, 1 M NaCl/0.1 % Tween 20, 3 M NaCl, and 3 M NaCl/0.1 % Tween 20 washes, respectively. Similarly, reintroducing the ZIKV MI smooth chips to ZIKV at 5.5 x 10^6 PFU/mL yielded average -ΔOCP responses of -1.16 ± 17.54 mV, 17.67 ± 18.38 mV, 76.39 ± 47.14 mV, and 67.05 ± 23.97 mV for the 1 M NaCl, 1 M NaCl/0.1 % Tween 20, 3 M NaCl, and 3 M NaCl/0.1 % Tween 20 washes, respectively. These tests were performed prior to determining that imprinting at 10^7 PFU/mL may be too high leading to analyte aggregation. Nevertheless, the rough and smooth MI chips exhibited a similar trend that the lower concentration of NaCl was ineffective for washing off the imprinted ZIKV virions. The next question was whether or not a 0.1 % Tween 20 solution was beneficial for washing off the imprinted analyte.

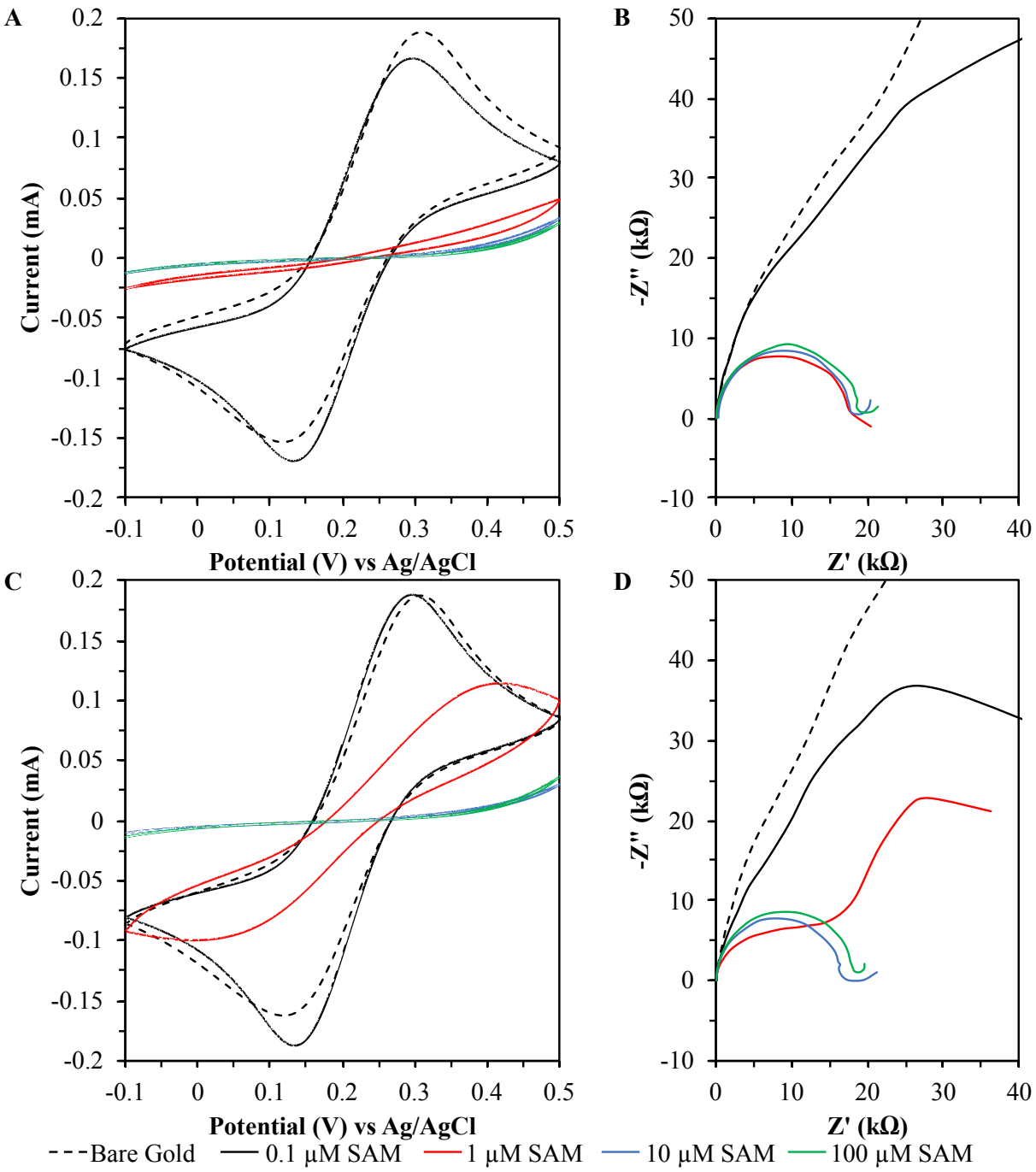

Fig. S5 Electrochemical analysis of alkanethiol SAM formation on gold chips. CV of the different electrodes: bare gold (dotted line), 0.1 µM thiol SAM (black line), 1 µM thiol SAM (red line), 10 µM thiol SAM (blue line), and 100 µM thiol SAM (green line) on rough (A) and smooth (C) gold chips: scan rate, 100 mV/s. EIS of the different electrodes: bare gold (dotted line), 0.1 µM thiol SAM (black line), 1 µM thiol SAM (red line), 10 µM thiol SAM (blue line), and 100 µM thiol SAM (green line) on rough gold chips (B) and smooth gold chips (D): 5 mV amplitude and frequency range of 0.1 – 100,000 Hz. Electrochemical analyses were performed in a KCl solution (0.1 M) containing $[Fe(CN)_6]^{4-}$/$[Fe(CN)_6]^{3-}$ (2 mM each).

The use of a higher salt concentration at 3 M NaCl proved to be effective at removing the imprinted ZIKV virions. However, the next concern was whether this high salt concentration or even the use of Tween 20 attacked the thiol SAM during the washing step of the MI process. Electrochemical analysis of these MI washing techniques was performed via CV. CV proved to be an effective tool at measuring and recording the thiol SAM formation on the gold chips. Again, chips were imprinted with thiol/DMSO in 10-fold serial dilutions ranging from 0.1 – 100 μM thiol for 2.5 hours. The thiol SAM chips were analyzed with CV and then washed with either 3 M NaCl or 3 M NaCl/0.1 % Tween 20 solutions overnight. CV of the washed thiol SAM chips demonstrated that a 3 M NaCl solution alone did not attack or alter the SAM on the chips. However, the 3 M NaCl solutions drastically decreased the electron transport of the SAM chips in combination with the Tween 20 solution. Comparing the CV of the 0.1 μM SAM chips before and after washing clearly demonstrated how Tween 20 effected the electrodes. The redox peaks completely disappear after washing the 0.1 μM SAM chips with Tween 20 (Fig. S7). Tween 20 is a nonionic detergent used mostly to remove attached proteins or DNA. Unfortunately, Tween 20 behaves like a surfactant and covered the exposed gold of the chips preventing the redox active metal ions from contacting the chip surface. Since the use of Tween 20 did not present a beneficial use in the washing technique, 3 M NaCl alone was chosen as the primary washing method for the MI process.

The next concern with the washing technique for the MI process was the large error yielded in the average potentiometric response of the ZIKV MI chips. 8 Rough gold chips were imprinted with ZIKV at 10^7 PFU/mL for 2.5 hours and then soaked in 3 M NaCl overnight to wash off the imprinted virions. 4 of those ZIKV MI chips were additional washed by soaking in DI H_2O for 30 minutes. The washed ZIKV MI chips were then reintroduced to ZIKV by pipetting serial dilutions of ZIKV from 1.2 x 10^1 to 5.5 x 10^6 PFU/mL into the detection system. The average -ΔOCP response for these MI chips are plotted in Fig. S8. When the ZIKV MI chips were reintroduced to ZIKV at 5.5 x 10^6 PFU/mL, the MI chips yielded average -ΔOCP responses of 24.43 ± 75.24 mV and 156.72 ± 22.26 mV for the 3 M NaCl and 3 M NaCl/DI H_2O washes, respectively. These results clearly demonstrate that there is salt residue on the MI chips after soaking in 3 M NaCl overnight. Washing this residue off significantly increases the reproducibility and precision of the ZIKV MI chip potentiometric response.

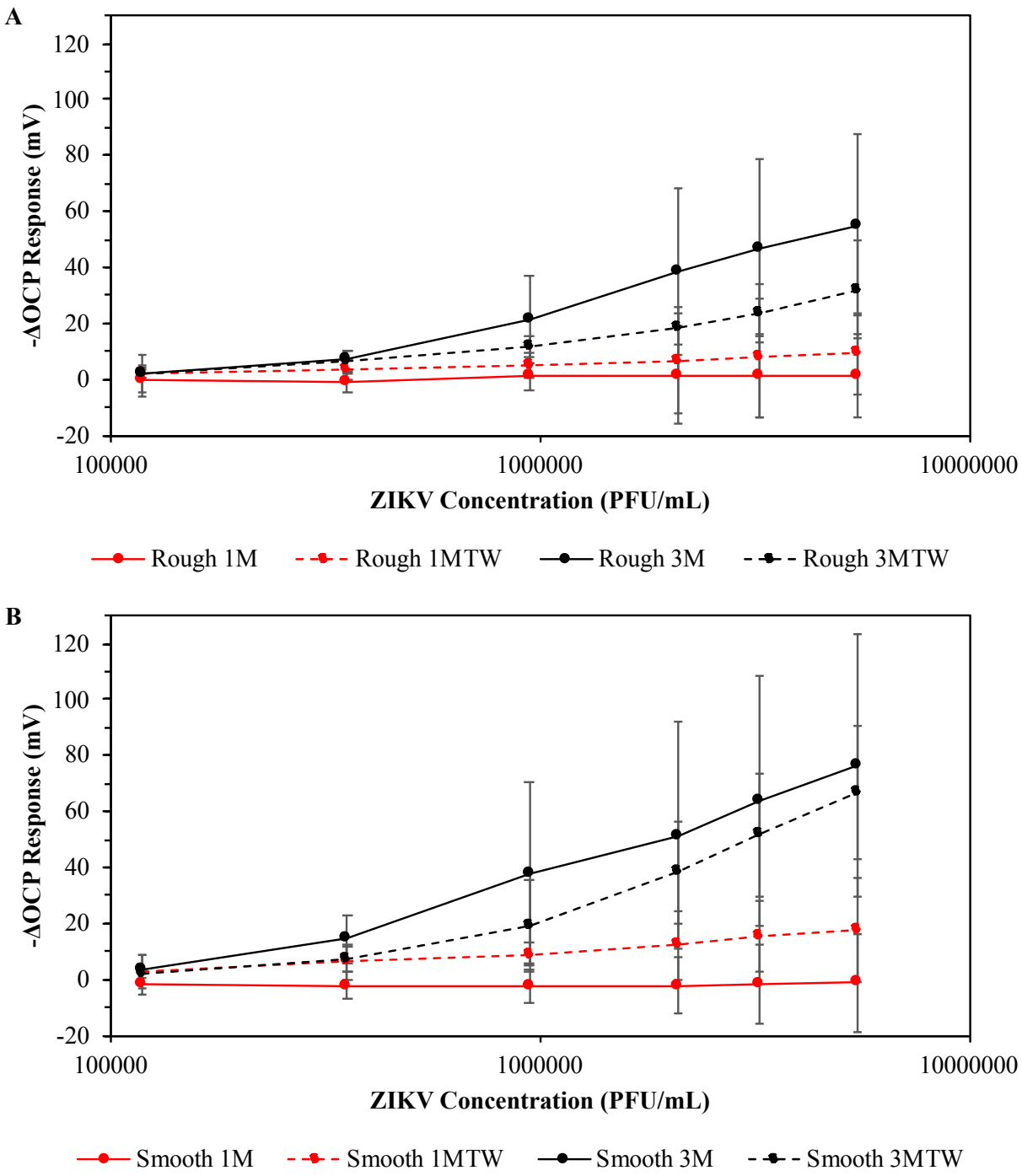

Fig. S6 Average Potentiometric responses of ZIKV re-adsorption on MI gold chips. Gold chips were imprinted with ZIKV at 10^7 PFU/mL on rough (A) and smooth (B) gold chips, washed with different solutions, including 1 M NaCl (1M), 1 M NaCl/0.1% Tween 20 (1MTW), 3 M NaCl (3M), and 3 M NaCl/0.1% Tween 20 (3MTW), then tested against ZIKV re-adsorption by measuring OCP response after adding serial dilutions of analyte to buffer in detection system.

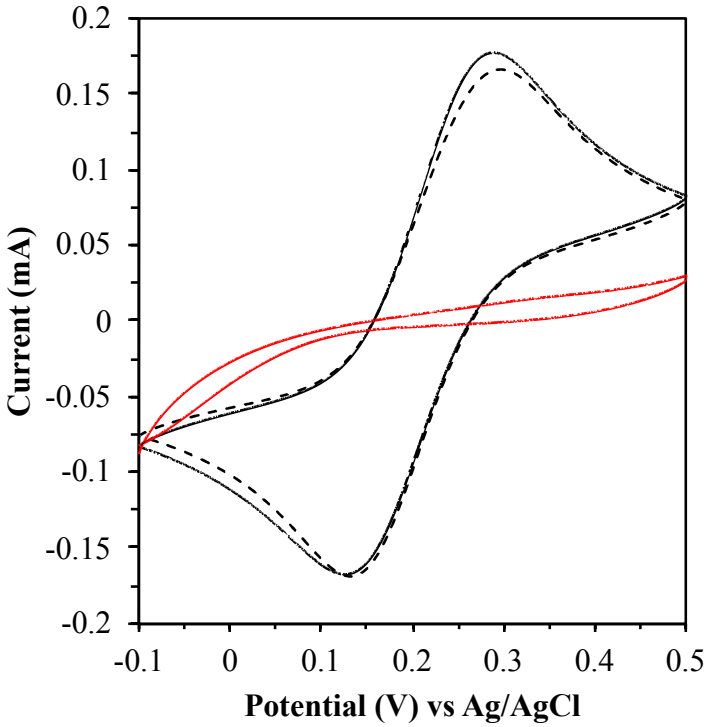

Fig. S7 Electrochemical analysis of MI washing technique with alkanethiol SAM on gold chips. Cyclic voltammograms of the different electrodes: 0.1 µM alkanethiol SAM (dotted line), 0.1 µM alkanethiol SAM washed overnight in (A) 3 M NaCl at 37°C/rocked (black line), and (B) 0.1 µM alkanethiol SAM washed overnight in 3 M NaCl/0.1% Tween 20 (red line) on rough gold chips: scan rate, 100 mV/s. Electrochemical analysis was performed in a KCl solution (0.1 M) containing $[Fe(CN)_6]^{4-}/[Fe(CN)_6]^{3-}$ (2 mM each).

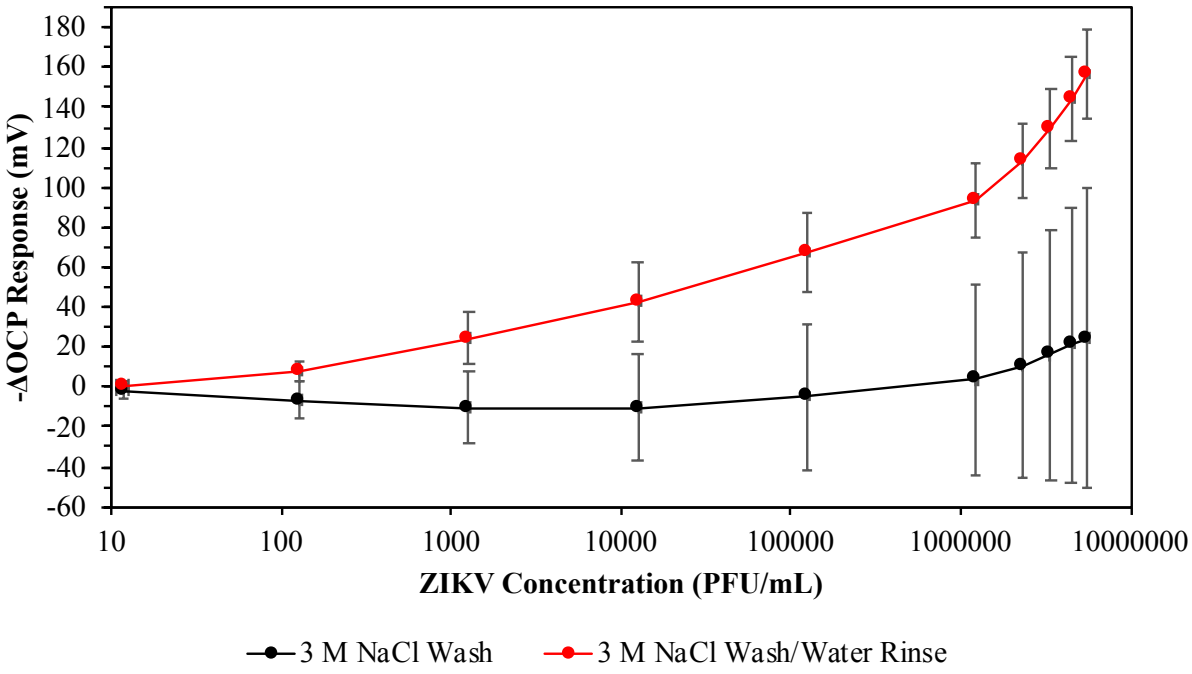

Fig. S8 Average Potentiometric responses of ZIKV re-adsorption on MI gold chips. Gold chips were imprinted with ZIKV at 10^7 PFU/mL on rough gold chips, washed with different solutions, including 3 M NaCl (black line) and 3 M NaCl followed by rinsing in DI H_2O (red line), then tested against ZIKV re-adsorption by measuring OCP response after adding serial dilutions of analyte to buffer in detection system.

S4 Real-time ZIKV detection in saliva

Human saliva is known to contain vast amounts of electrolytes, enzymes, proteins, bacteria, and cells.[7] Human saliva was collected from a single volunteer, with no known history of ZIKV infection through an IRB-approved protocol. The collected saliva was kept in its natural state in order to test the precision of the lock-and-key complexes on the MI chips. 6 rough chips were imprinted with ZIKV at 10^4 PFU/mL for 2.5 hours. The MI chips were soaked in 3 M NaCl overnight to wash off the imprinted virions and then soaked in DI H_2O for 30 minutes. 3 of the washed ZIKV MI chips were introduced to pure saliva by pipetting aliquots of saliva into the detection system. In order to test the selectivity of this 3D MI detection system, the collected saliva was doped with ZIKV with a final concentration of 4 x 10^4 PFU/mL to match a clinical viral load of ZIKV in saliva.[8] The remaining washed ZIKV MI chips were then reintroduced to ZIKV by pipetting aliquots of the 4 x 10^4 PFU/mL ZIKV-doped saliva into the detection system. The real-time potentiometric responses of 1 of the ZIKV MI chips tested against saliva and 1 of the ZIKV MI chips tested against ZIKV-doped saliva is plotted in Fig. S9. When the ZIKV MI chips were introduced to the analytes at a total volume of 2 µL added into the detection system after providing 20 minutes for the detection system to equilibrate, the MI chips yielded a ΔOCP response of 23.72 mV and -43.51 mV from pure saliva and ZIKV-doped saliva, respectively, after 5 additional minutes of assay time. After adding a total volume of 4 µL of the analytes into the detection system, the MI chips yielded a total ΔOCP response of 31.05 mV and -69.63 mV from pure saliva and ZIKV-doped saliva, respectively, after another additional 5 minutes of assay time.

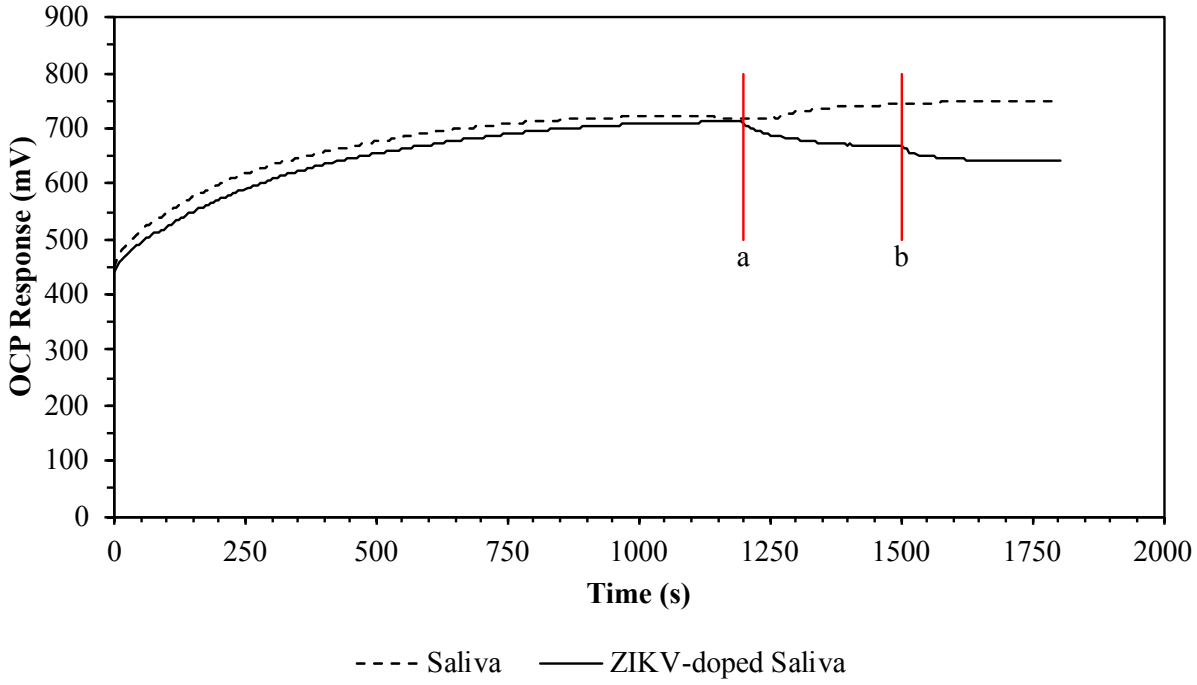

Fig. S9 Real-time potentiometric responses on MI gold chips. Gold chips were imprinted with ZIKV at 10^4 PFU/mL in buffer on rough gold chips. Real-time potentiometric cross-test of ZIKV MI chip against pure saliva (dotted line) and potentiometric test of ZIKV MI chip against ZIKV re-adsorption (solid line). Samples were added to the detection system at 1200 s (a) and at 1500 s (b) with either 2 µL of pure saliva or 2 µL of ZIKV-doped saliva at 4 x 10^4 PFU/mL.

References

1. Y. Yu, Q. Zhang, J. Buscaglia, C.-C. Chang, Y. Liu, Z. Yang, Y. Guo, Y. Wang, K. Levon and M. Rafailovich, *Analyst*, 2016, **141**, 4424-4431.
2. M. Cohen-Atiya and D. Mandler, *Journal of Electroanalytical Chemistry*, 2003, **550-551**, 267-276.
3. Y. Yu, Q. Zhang, C.-C. Chang, Y. Liu, Z. Yang, Y. Guo, Y. Wang, D. K. Galanakis, K. Levon and M. Rafailovich, *Analyst*, 2016, **141**, 5607-5617.
4. J. C. Love, L. A. Estroff, J. K. Kriebel, R. G. Nuzzo and G. M. Whitesides, *Chemical Reviews*, 2005, **105**, 1103-1170.
5. N. Elgrishi, K. J. Rountree, B. D. McCarthy, E. S. Rountree, T. T. Eisenhart and J. L. Dempsey, *Journal of Chemical Education*, 2018, **95**, 197-206.
6. E. P. Randviir and C. E. Banks, *Analytical Methods*, 2013, **5**, 1098-1115.
7. M. Tiwari, *Journal of Natural Science, Biology, and Medicine*, 2011, **2**, 53-58.
8. L. Barzon, M. Pacenti, A. Berto, A. Sinigaglia, E. Franchin, E. Lavezzo, P. Brugnaro and G. Palù, *Eurosurveillance*, 2016, **21**.